



## Catalytic ozonation of clofibric acid over copper-based catalysts: In situ ATR-IR studies



Shailesh S. Sable<sup>a</sup>, P.P. Ghute<sup>a</sup>, D. Fakhrnasova<sup>a</sup>, R.B. Mane<sup>b</sup>, C.V. Rode<sup>b</sup>, F. Medina<sup>a</sup>, S. Contreras<sup>a,\*</sup>

<sup>a</sup> Departament d'Enginyeria Química, Universitat Rovira i Virgili, Av. Països Catalans 26, 43007 Tarragona, Spain

<sup>b</sup> Chemical Engineering and Process Development Division, CSIR-National Chemical Laboratory, Pune 4110008, India

### ARTICLE INFO

#### Article history:

Received 14 October 2016

Received in revised form 19 January 2017

Accepted 21 February 2017

Available online 6 March 2017

#### Keywords:

Catalytic ozonation

Clofibric acid

Cu-catalysts

Mechanism

In situ ATR-IR

### ABSTRACT

The current study describes the catalytic ozonation of clofibric acid (CFA) under ambient conditions using copper oxide catalysts synthesized by different methods. The objective of this study is to provide novel catalysts and reaction mechanism for the degradation of emerging pharmaceutical compounds in aqueous solution. Among the various Cu catalysts screened in this study, the Cu<sub>1</sub>–Al<sub>1</sub> oxide catalyst showed an excellent activity and stability in the degradation and mineralization of CFA. In situ attenuated total reflection IR (ATR-IR) spectroscopy was used to examine the interaction of ozone with the active sites of the catalyst in presence of water and to investigate the possible catalytic mechanism. The presence of Lewis acid sites in the Cu<sub>1</sub>–Al<sub>1</sub> catalyst increased the amount of chemisorbed water enhancing stronger interaction of ozone to form surface activated species, resulting in higher catalytic activity. The results obtained from in-situ ATR-IR study indicate that surface hydroxyl groups and Lewis acid sites are responsible for promoting the generation of hydroxyl radicals (OH<sup>•</sup>) from aqueous ozone.

© 2017 Elsevier B.V. All rights reserved.

## 1. Introduction

Degradation of emerging organic pollutants by oxidation using heterogeneous catalysis is considered to be one of the most effective techniques for water remediation [1,2]. Pharmaceutical compounds are among the group of emerging pollutants, because their noxious effects even at very low concentration have occasioned a big concern. Due to the incomplete sewage treatment, every year a large number of pharmaceuticals and personal care products (PPCPs) enter in the environment. PPCPs are now recognized as a new class of emerging environmental contaminants and bring increasing concern and scientific interest [3–5].

Pharmaceutical compounds like lipid regulators have been found in different aquatic environments [6–8]. They have been detected in the natural water systems of various European countries like Spain [9], Switzerland [10], England [11] and also found in the Nord Sea [12]. The large discharge of lipid regulators in the environment produces lasting adverse effects on living beings because of incomplete removal by wastewater treatment plants (WWTPs) [13–15]. Clofibric acid (CFA) is a lipid regulator that has shown high

persistence in water and it has been found in surface water, groundwater and even drinking water [16–25]. CFA has been found in STP effluents and various sources of water showing high persistency in the environment [26–28]. Advanced Oxidation Processes (AOPs) could be interesting and effective technologies for the removal of these type of recalcitrant contaminants.

AOPs involve the generation of hydroxyl radicals which are effective for the removal of organic pollutants from wastewater [29]. Ozone is used in water treatment process because of its powerful oxidation capacity [30–35]. However, as it has been reported in several cases, ozonation can not completely degrade organic compounds and sometimes produce more toxic intermediates. Ozone can be combined with H<sub>2</sub>O<sub>2</sub> or UV irradiation to generate free radicals, however they present some drawbacks such as residual of H<sub>2</sub>O<sub>2</sub> [36], and high energy consumption of UV lamp [37].

Catalytic ozonation is known as an effective AOPs to remove organic pollutants from wastewaters. Although single ozonation is not sufficient for the complete oxidation of recalcitrant organic compounds, they can be successfully oxidized by catalytic ozonation [36–40]. Supported and unsupported metals and metal oxides are used in the ozonation of organic compounds in water [41]. Copper, nickel, iron, cobalt containing transition metals were used in ozonation process, showing improvement in TOC removal by ozone decomposition and hydroxyl radicals generation [42–44]. In sev-

\* Corresponding author.

E-mail address: [sandra.contreras@urv.cat](mailto:sandra.contreras@urv.cat) (S. Contreras).

eral cases, alumina-supporting metal oxides of Fe, Ag, Co, Ni, Mn and Cu have shown high activity for the destruction of pollutants with ozone [45–47].

Removal of pharmaceutical compounds/emerging contaminants using mesoporous nanocrystalline MgO nanoparticle, magnetic Fe<sub>3</sub>O<sub>4</sub> nanoparticles, iron silicate loaded pumice in catalytic ozonation have been reported [48–50]. Aqueous solutions of clofibric acid (CFA) have been treated by catalytic ozonation using copper based dawsonite and hydrotalcite-like catalysts [51,52].

Typically, the successful catalytic ozonation requires the adsorption of ozone, organic molecules or both on the catalyst surface and the enhanced generation of OH radicals.

The activity of the catalysts mentioned is based mainly on promotion of catalytic ozone decomposition and the enhanced generation of hydroxyl radicals. However, results obtained from various studies suggest differently catalytic ozonation mechanisms.

Although there are some previous studies available in the literature, the mechanism of catalytic ozonation with solid materials is not yet well understood, neither the active species involved. Techniques like isotopic substitution and in situ Raman spectroscopy were used to study the ozone decomposition mechanism in gas phase [53,54]. Previous studies proposed that the formation of different species like superoxide or peroxide species via redox process occurs on the surface of the metal oxide. On weak Lewis sites, the formation of hydrogen bonds with surface OH groups is observed, whereas on strong Lewis sites the ozone interaction resulted in the formation of atomic oxygen atoms [55]. Metal oxides in presence of water adsorb water molecule, which dissociates into OH<sup>-</sup> and H<sup>+</sup>, and surface hydroxyl group formation occurs with oxygen sites and surface metal. At pH values above the isoelectric point, the predominate surface species is M-O<sup>-</sup>, while at pH values below the isoelectric point, M-OH<sub>2</sub><sup>+</sup> species predominate. These species can act as an initiator of a chain reaction involving the decomposition of ozone, leading to the formation of hydroxyl radicals [55–58]. Previous studies of mechanism suggested that catalytic ozonation in presence of metal oxide can proceed through two pathways: (i) promotion of hydroxyl radical generated from aqueous ozone [56,59,60] and (ii) surface complexes formation between the carboxylic groups of the pollutants and the surface metal sites of the catalysts [61–63]. In aqueous phase, decomposition of ozone depends on the ability of the catalyst to adsorb and desorb O<sub>3</sub>, the activity of the oxygen species, and the ability to desorb O<sub>2</sub> [64].

*In situ* detections of trace amounts of adsorbed/deposited surface species at the solid-liquid interface require sophisticated spectroscopic techniques with very high signal-to-noise ratio. Attenuated total reflection infrared (ATR-IR) spectroscopy is known to be a powerful method to selectively extract information on intermediate species at the catalytic solid-liquid interface. This technique provides key fundamental information about surface bound species in catalytic reactions, which would provide information on both reaction mechanisms and the nature of the solids used as catalysts. Therefore, an understanding of catalytic performance and surface species present during catalytic ozonation can be investigated using *in situ* ATR-IR spectroscopy.

This work is focused on the development of novel and stable catalytic materials for the abatement of emerging contaminants. In the present study, we investigate the ability of different copper-based catalysts for the degradation of clofibric acid (CFA) by ozonation. The identification of the degradation products of the catalytic ozonation of CFA with dawsonite-type catalysts as well as a proposal of the reaction mechanism was presented in a previous study [51]. In this work, the catalytic activity and surface changes of catalyst before and after the ozonation process was studied by *in situ*

ATR-IR spectroscopy to obtain a new insight about the catalytic mechanism.

## 2. Experimental

### 2.1. Catalysts preparation

Three kinds of copper based catalysts were synthesized by different methods.

[I] *Cu-dawsonite catalysts*: Copper dawsonites with Cu/Al mass ratios 0 (NH<sub>4</sub>DW), 0.02 (Cu<sub>2</sub>DW) and 0.1 (Cu<sub>10</sub>DW) were obtained by co-precipitation method at constant pH. The procedure is detailed in a previous reference [51].

[II] *Cu-hydrotalcite-like catalysts*: Cu containing Mg/Al hydrotalcite (HT) catalysts and spinel-type catalysts CuMg<sub>x</sub>Al<sub>2</sub>O<sub>4</sub> and Cu<sub>x</sub>Al<sub>2</sub>O<sub>4</sub> were synthesized by co-precipitation method, and calcined for 6 h at different temperatures. The detailed procedure is described in reference [52].

[III] *Cu<sub>1</sub>-Al<sub>1</sub> catalyst*: Cu<sub>1</sub>-Al<sub>1</sub> catalyst was synthesized by a co-precipitation method with the simultaneous addition of Cu(NO<sub>3</sub>)<sub>2</sub>·3H<sub>2</sub>O, Al(NO<sub>3</sub>)<sub>3</sub>·9H<sub>2</sub>O (0.05 M) and aqueous K<sub>2</sub>CO<sub>3</sub> (0.2 M) in 5–10 mL of water at room temperature. Digestion was carried out for 4–5 h and then filtered and washed with deionized water and dried at 100 °C for 5–8 h and further calcined at 400 °C for 4 h [65].

### 2.2. Catalysts characterization

ICP-OES (SPECTRO-ARCOS FHS16) was used for measurement of metal content in copper based catalyst. XRD and N<sub>2</sub> physisorption method was used to study the structure of the catalysts. Rigaku, D-max III VC model with nickel filtered CuK $\alpha$  radiation was used for X-ray powder diffraction measurement. The samples were scanned in the 2 $\theta$  range of 1.5–80°. N<sub>2</sub> adsorption was performed using a Micromeritics ASAP 2010 apparatus at 77 K. Before analysis, the samples were degassed at 120 °C for 12 h. Autosorb 1100 instrument was used for Temperature programmed desorption (TPD) measurements. Ammonia TPD measurements were carried out by: (i) pre-treating the samples from room temperature to 673 K for 20–30 min under helium flow rate of 65 mL/min, (ii) adsorption of ammonia (5%) at 80 °C and (iii) desorption of adsorbed ammonia with a heating rate of 15 °C min<sup>-1</sup> starting from 353 K to 973 K, to evaluate the acidity of the catalysts.

A pyridine-IR spectrum was recorded on PerkinElmer frontier instrument having Harrick Diffuse reflectance assembly with temperature controller under 150 mL/min flow of nitrogen as carrier gas. 20 mg of catalyst was filled in a sample cup and 40 mL of pyridine in gas phase was injected in a N<sub>2</sub> flow. Then the physisorbed pyridine was removed by a N<sub>2</sub> flow at 90 °C. Desorption of pyridine was recorded in the temperature range of 30–200 °C. X-Ray photoelectron spectroscopy (XPS) data were collected on a VG Scientific ESCA-3000 spectrometer using a non-monochromatized Mg K $\alpha$  radiation (1253.6 eV) at a pressure of about 1 × 10<sup>-9</sup> Torr (pass energy of 50 eV, electron take off angle 55°) and overall resolution ~0.7 eV determined from the full width at half maximum of the 4f<sub>7/2</sub> core level of the gold surface. The error in the binding energy values were within 0.1 eV. The binding energy values were charge-corrected to the C<sub>1s</sub> signal (285.0 eV) [65].

*In situ* ATR-IR spectroscopy was employed to monitor the surface species of the catalyst materials under similar experimental conditions of the ozonation reaction. A catalyst material in the powder form (ca.50 mg) was suspended in ethanol and was deposited over ZnSe internal reflection element (IRE) by slowly dropping the suspension with a subsequent drying process. The ZnSe IRE was mounted in an accessory (PIKE Technologies, HATR Htd Flow-Thru

Cell) and aqueous solution containing ozone, CFA, and/or phosphoric acid was passed through the cell. The cell was amounted in an IR spectrometer (Brucker, Tensor 27) with a DTGS detector. Infrared spectra over the 800–4000 cm<sup>-1</sup> range were recorded with a resolution of 4 cm<sup>-1</sup> at room temperature.

### 2.3. Experimental procedure

The ozonation experiments were conducted in a 1.5 L glass reactor containing aqueous solution of CFA (10–100 mg/L, 500 mL) at ambient conditions ( $25 \pm 2^\circ\text{C}$ ) and atmospheric pressure. Higher concentrations than those commonly found in wastewaters were used to compare the efficiency of the different catalysts tested and to favour the accuracy in the analytical determinations. 250 mg of catalyst was added in aqueous solution of CFA and 1.2 g/h of O<sub>3</sub> passed through the solution generated by an ozone generator (ANSEROS COM-AD-02) from pure O<sub>2</sub> (40 L/h). The samples were taken periodically for analysis. CFA concentrations were measured by high performance liquid chromatography HPLC (Shimadzu LC-2010 equipped with a SPD-M10A Diode array UV-vis detector) at wavelength 254 nm. A Varian OmniSphere C18 column and a solution containing an aqueous buffer (Milli-Q H<sub>2</sub>O 1 L, methanol 50 mL and H<sub>3</sub>PO<sub>4</sub> 4 mL) and acetonitrile (40:60) was used as mobile phase. Shimadzu 5000-A TOC analyzer was used for TOC measurements.

## 3. Results and discussion

### 3.1. Catalysts characterization

Table 1S (see Supplementary Information) shows the textural properties, BET specific surface area, pore volume and Cu content of Cu-dawsonite, Cu-hydrotalcite and Cu<sub>1</sub>–Al<sub>1</sub> catalysts. Surface area and pore volume of Cu<sub>2</sub>DW, Cu<sub>10</sub>DW and Cu<sub>10</sub>DW (500) were 426, 338, 297 m<sup>2</sup> g<sup>-1</sup> and 0.954, 0.632, 0.964 ccg<sup>-1</sup>, respectively, whereas surface area and pore volume of Mg<sub>3</sub>Cu<sub>0.5</sub>Al<sub>1</sub> (900) hydrotalcite was 92 m<sup>2</sup> g<sup>-1</sup> and 0.035 ccg<sup>-1</sup>, respectively. An important decrease of the surface area of the dawsonite samples was observed when the amount of copper in the sample increased, besides a decrease of the pore volume of the samples. When calcined at higher temperature (900 °C) a decrease in the surface area was observed, suggesting that porous structure originated from the initial structure collapsed and the crystallization of spinel phase progress. Hence, all calcined spinel type materials show very low surface area. Surface area and pore volume of calcined Cu<sub>1</sub>–Al<sub>1</sub> (400) catalyst was 74 m<sup>2</sup> g<sup>-1</sup> and 0.60 m<sup>3</sup> g<sup>-1</sup> respectively. Among all copper catalysts, Cu<sub>2</sub>DW possesses the highest surface area (426 m<sup>2</sup> g<sup>-1</sup>) whereas spinel Cu<sub>1</sub>Al<sub>2</sub>O<sub>4</sub> (900) catalyst possesses the lowest (13 m<sup>2</sup> g<sup>-1</sup>) surface area (see Table 1S).

XRD phases of all copper catalysts are shown in Table 2S. For copper spinel-type catalysts, tenorite and spinel were detected as main phases. Mg<sub>3</sub>Cu<sub>0.5</sub>Al<sub>1</sub> (900) hydrotalcite shows spinel, tenorite and periclase crystalline phases. The spinel (MgAl<sub>2</sub>O<sub>4</sub> or CuAl<sub>2</sub>O<sub>4</sub>) phase appeared together with small amount of tenorite phase (CuO) in Cu<sub>0.25</sub>Mg<sub>0.75</sub> Al<sub>2</sub>O<sub>4</sub> (900) catalyst. XRD patterns of the Cu-dawsonite catalysts are shown in Fig. 1S. The XRD patterns of synthesized catalyst are consistent with the characteristic diffractions of ammonium dawsonite (NH<sub>4</sub>Al(CO<sub>3</sub>)(OH)<sub>2</sub>, JCPDS 01-076-1923). The XRD pattern of the Cu<sub>10</sub>DW(500) shows the disappearance of the dawsonite phase and the formation of an amorphous phase. XRD patterns of the calcined Cu<sub>1</sub>–Al<sub>1</sub> catalyst are shown in Fig. 2S. The existence of CuO [(111) JCPDS file no. 80-1268] and CuAl<sub>2</sub>O<sub>4</sub> [(222) JCPDS file no. 73-1958] phases were confirmed by a broad diffraction peak at  $2\theta = 35.7^\circ$  and  $38.8^\circ$ , respectively.

Among all Cu based catalysts Cu<sub>1</sub>–Al<sub>1</sub> showed excellent catalytic activity in this process. Therefore, a more complete characterization of this catalyst was performed.

XPS analysis were carried out to study the surface chemistry of this catalyst. C (1s) (285.0 eV) and O (1s) (530 eV) were used as the reference to calibrate binding energies. The Cu 2p XPS of the calcined Cu<sub>1</sub>–Al<sub>1</sub>(400) catalyst are shown in Fig. 3S(a). A broad peak observed in the range of 930–937 eV, confirm the presence of various Cu species. The wide Cu 2p<sub>3/2</sub> signals obtained for this catalyst could be fitted satisfactorily to two principal peaks after deconvolution, as shown in Fig. 3S(b). The predominant peak at 933.6 eV belongs to Cu<sup>2+</sup> of CuO, which is formed during calcination process. Interestingly, another peak appears at 935 eV in Fig. 3S(b) and it is also attributed to Cu<sup>2+</sup>, but from spinel CuAl<sub>2</sub>O<sub>4</sub> phase. A satellite peak at 940–946 eV was also observed (Fig. 3S(a)), indicating the presence of Cu<sup>2+</sup> in the form of CuO and CuAl<sub>2</sub>O<sub>4</sub>. Fig. 4S shows O 1s and Al 2p XPS spectra of the calcined Cu<sub>1</sub>–Al<sub>1</sub> catalyst. The peak at 530.3 eV belongs to binding energy of O 1s, which is correlated to CuO. And the peak at 73.6 eV is attributed to binding energy of Al, which is correlated to Al<sub>2</sub>O<sub>3</sub>. The XPS of Al shows a shoulder at around 77 eV that is associated to the interference of Cu 3p (see Fig. 4S).

H<sub>2</sub>-TPR of calcined Cu<sub>1</sub>–Al<sub>1</sub> catalyst was studied and shown in Fig. 5S. A single broad peak of calcined catalyst was observed in the region of 180–400 °C, due to the reduction of CuO to copper in one step.

TEM analysis of the Cu<sub>1</sub>–Al<sub>1</sub> catalyst was performed, showing metal particles of ca. 10 nm, and showing the characteristic diffraction planes (110), (111), (311) and (204) of the CuO phase [65].

The ammonia temperature-programmed desorption (NH<sub>3</sub>-TPD) is one of the most conventional methods for characterizing acidity of catalysts. The strength and natures of acid sites of the calcined Cu<sub>0.75</sub>Mg<sub>0.25</sub>Al<sub>2</sub>O<sub>4</sub>, Cu<sub>1</sub>Al<sub>2</sub>O<sub>4</sub> and Cu<sub>1</sub>–Al<sub>1</sub> catalysts were determined by NH<sub>3</sub>-TPD and shown in Fig. 6S. A low NH<sub>3</sub> desorption peak is observed for all the samples between 120–300 °C. For Cu<sub>0.75</sub>Mg<sub>0.25</sub>Al<sub>2</sub>O<sub>4</sub> and Cu<sub>1</sub>Al<sub>2</sub>O<sub>4</sub> samples, a small desorption peak is also observed at around 580 °C. The NH<sub>3</sub>-TPD peak for calcined Cu<sub>1</sub>–Al<sub>1</sub> catalyst appeared at 190 and 530 °C. Notably, for the Cu<sub>1</sub>–Al<sub>1</sub> catalyst an important desorption of NH<sub>3</sub> was detected between 400–700 °C, indicating the presence of strong acid sites (see Fig. 6S). Furthermore, the amount of NH<sub>3</sub> desorbed was significantly higher for Cu<sub>1</sub>–Al<sub>1</sub> catalyst, revealing that it presents more acidic sites than the other two catalysts. Therefore, calcined Cu<sub>1</sub>–Al<sub>1</sub> catalyst shows the highest acidity among all the three Cu-based catalysts analyzed.

To know the nature of the acid sites of calcined Cu<sub>1</sub>–Al<sub>1</sub> catalyst, pyridine adsorption–desorption study was performed in the temperature range of 100–375 °C. Fig. 7S shows the expected bands due to hydrogen-bonded pyridine at 1430 cm<sup>-1</sup> and Lewis acid-bound pyridine at 1455, 1588, and 1623 cm<sup>-1</sup>. A band observed at 1546 cm<sup>-1</sup> confirmed the presence of Brønsted acid sites and the band at 1646 cm<sup>-1</sup> is attributed to pyridine bound on Brønsted acid sites. The band at 1496 cm<sup>-1</sup> is attributed to pyridine associated with both Lewis and Brønsted acid sites [66].

### 3.2. Clofibric acid (CFA) degradation and mineralization

**Table 1** shows the TOC removal during ozonation of CFA by various Cu-based catalysts. Furthermore **Table 1** also shows the Cu leached after 2 h of reaction. When the reaction was performed using single ozonation (without catalyst) a 100% CFA conversion was observed in 15 min (0.1 mg/L-detection limit). However, the degree of mineralization was not higher than 28% and 40% after 2 h and 6 h of reaction, respectively. Similar to single ozonation, the Cu-derived catalysts also showed completed CFA conversion within 15 min. However enhancement in TOC removal was observed,

**Table 1**

CFA degradation results using different Cu-based catalysts after 2 h of single and catalytic ozonation.

Catalysts	%TOC Removal	Cu (mg/L) Leaching
O <sub>3</sub>	28.1	–
I-Cu <sub>2</sub> DW	55.2	0.5
I-Cu <sub>10</sub> DW	67.3	1.3
I-Cu <sub>10</sub> DW (500)	57.9	3.4
II-Mg <sub>3</sub> Cu <sub>0.5</sub> Al <sub>1</sub> (900)	60.0	2.1
II-Cu <sub>0.75</sub> Mg <sub>0.25</sub> Al <sub>2</sub> O <sub>4</sub> (900)	55.3	1.6
II-Cu <sub>1</sub> Al <sub>2</sub> O <sub>4</sub> (900)	50.0	2.4
II-Cu <sub>0.75</sub> Mg <sub>0.25</sub> Al <sub>2</sub> O <sub>4</sub> (2%OA, 900)	54.4	0.7
II-Cu <sub>1</sub> Al <sub>2</sub> O <sub>4</sub> (2%OA, 900)	53.3	1.1
III-Cu <sub>1</sub> -Al <sub>1</sub>	81.7	–
Cu <sup>2+</sup> (3.5 mg/L)	38.3	–

Reaction conditions: 500 mL, [CFA]<sub>0</sub> = 100 mg/L, O<sub>3</sub> production = 1.2 g/h, O<sub>2</sub> flow rate = 40 L/h, catalyst concentration = 0.5 g/L, Temp. = R.T., pH = free and time = 2 h.

achieving more than 50% mineralization in 2 h of catalytic ozonation using Cu-catalysts. Copper dawsonite (I) catalysts show good performance in clofibric acid mineralization using Cu<sub>2</sub>DW, Cu<sub>10</sub>DW and Cu<sub>10</sub>DW(500), achieving 55.7 and 58% of mineralization in 2 h, respectively. The use of the calcined catalyst Cu<sub>10</sub>DW (500) shows decrease in the activity, compared with the non-calcined catalysts (Cu<sub>2</sub>DW, Cu<sub>10</sub>DW). Nevertheless, between 0.5–3.3 mg/L of Cu was leached during the reaction (see Table 1) for as-synthesized and calcined Cu-dawsonite catalysts. When the amount of copper in the catalytic material increased, the amount of Cu leached also increased. Cu-HT/spinel-type (II) catalysts also show good performance in catalytic ozonation of clofibric acid. When using Mg<sub>3</sub>Cu<sub>0.5</sub>Al<sub>1</sub> hydrotalcite, Cu<sub>1</sub>Al<sub>2</sub>O<sub>4</sub> and Cu<sub>0.75</sub>Mg<sub>0.25</sub>Al<sub>2</sub>O<sub>4</sub> spinel catalysts (calcined at 900 °C), a 50, 55 and 60% degree of mineralization was achieved respectively, but with 2.4, 1.6 and 2.1 mg/L of Cu leaching, respectively, after 2 h of ozonation (see Table 1). The amount of Cu leached for these samples is too high, and this could involve problems of toxicity in the effluents. In order to solve this problem and with the aim to decrease the amount of Cu leached, probably due to the presence of CuO phase (tenorite phase), the sample was treated with an aqueous solution of 2% oxalic acid and then calcined at 900 °C. Then the catalysts were tested as well in the catalytic ozonation reaction and leaching tests were carried out. After pretreatment with oxalic acid and removal of the excess phases, these pure copper spinel type catalysts lead to a decrease in the amount of Cu leached (1.1 mg/L – Cu<sub>1</sub>Al<sub>2</sub>O<sub>4</sub> and 0.7 mg/L – Cu<sub>0.75</sub>Mg<sub>0.25</sub>Al<sub>2</sub>O<sub>4</sub>) while maintaining ca. 55% mineralization after 2 h of ozonation (see Table 1).

The Cu<sub>1</sub>-Al<sub>1</sub> catalyst obtained best performance, achieving 82% TOC removal in 2 h of ozonation with no leaching of Cu (see Table 1). When ozonation experiment with this Cu<sub>1</sub>-Al<sub>1</sub> catalyst was further carried out for 6 h, 96% mineralization was obtained. This catalyst showed then to be highly active and stable under the tested conditions.

Test of adsorptions were also carried out with all catalysts, showing negligible adsorption of CFA (results not shown).

### 3.3. Contribution of homogeneous mechanism due to leached Cu

No leaching of copper was observed using Cu<sub>1</sub>-Al<sub>1</sub> catalyst for CFA degradation, but with Cu-dawsonite and Cu-HT and spinel type catalysts, up to 3.3 and 2.4 mg/L of Cu leaching was observed, respectively (see Table 1). To check the contribution of dissolved metal (Cu<sup>2+</sup>) in the reaction system, an ozonation experiment was carried out with 3.5 mg/L of copper concentration (dissolved Cu<sup>2+</sup>). The results of this experiment are shown in Table 1, and a slight improvement was observed in TOC removal when compared to single ozonation. Total CFA removal was also produced within 15 min. Therefore, it can be said that dissolved copper can slightly enhance

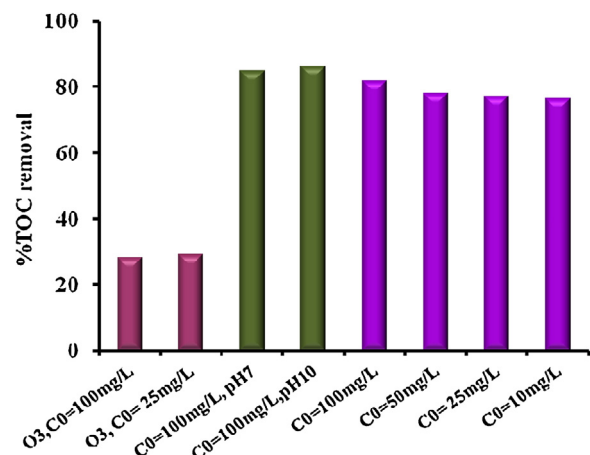


**Fig. 1.** Degree of mineralization obtained in 2 h ozonation with different concentration of CFA and initial pH using Cu<sub>1</sub>-Al<sub>1</sub> (0.5 g/L) catalyst.

the ozonation process, as 10% contribution in mineralization was observed with 3.5 mg/L of Cu.

### 3.4. Reuse and recycling of Cu<sub>1</sub>-Al<sub>1</sub> catalyst

Calcined Cu<sub>1</sub>-Al<sub>1</sub> catalyst have shown best performance in ozonation, achieving mineralization degrees of 82% and 96% after 2 and 6 h, respectively. To check the stability of this catalyst, reactions were performed in the presence of Cu<sub>1</sub>-Al<sub>1</sub> catalyst recovered after reaction and reused in 3 consecutive runs of catalytic ozonation, as shown in Fig. 8S. Complete (under our detection limit 0.5–0.1 mg/L) removal of CFA was observed within 15 minute, same as fresh catalysts. From the results it can be seen that catalytic activity of this catalyst was maintained, as they show near about 76–78% TOC removal after being used for three consecutive cycles, which demonstrate the good stability of this catalyst. The highest activity and stability of the Cu<sub>1</sub>-Al<sub>1</sub> catalyst can probably be attributed to the stable and well dispersed active metal species (XRD show lower crystallinity, suggesting higher dispersion of copper oxide phases). Cu<sub>1</sub>-Al<sub>1</sub> possess higher Cu content compared to CuDW and Cu-HT-spinel type catalysts and also, higher surface area when compared to spinel catalysts (see Table 1S). From XRD and XPS results, highly dispersed spinel CuAl<sub>2</sub>O<sub>4</sub> and CuO phases are formed in the Cu<sub>1</sub>-Al<sub>1</sub> catalyst, probably due to the protocol preparation. Also, the NH<sub>3</sub>-TPD results show higher acidity for Cu<sub>1</sub>-Al<sub>1</sub> catalyst when compared to the other copper catalysts. This fact may play a crucial role in the catalytic performance.

### 3.5. Tests with lower CFA concentration and different initial pH

To check the efficiency of the Cu<sub>1</sub>-Al<sub>1</sub> catalyst under different operating conditions, experiments were performed using low concentrations of CFA and different initial pHs. Fig. 1 shows the degree of mineralization after 2 h of single and catalytic ozonation process with Cu<sub>1</sub>-Al<sub>1</sub> catalyst, in reactions performed with different CFA initial concentrations (10, 25 and 50 mg/L) at free pH. In all cases, total CFA removal occurred within 15 min reaction, below our detection limit (0.1 mg/L). It was observed that Cu<sub>1</sub>-Al<sub>1</sub> catalyst also showed good performance with low concentration of CFA. When catalytic ozonation experiments were performed using 10 mg/L, 25 mg/L and 50 mg/L of initial CFA concentration at free pH, 76%, 77% and 79% degree of mineralization was achieved, respectively, in 2 h. The effect of the pH was also studied in catalytic ozonation with 100 mg/L of CFA at initial pH 7 and 10 (not buffered). Total conversion of CFA was observed within 10 min of reaction with an improvement in mineralization, achieving 85 and 87%

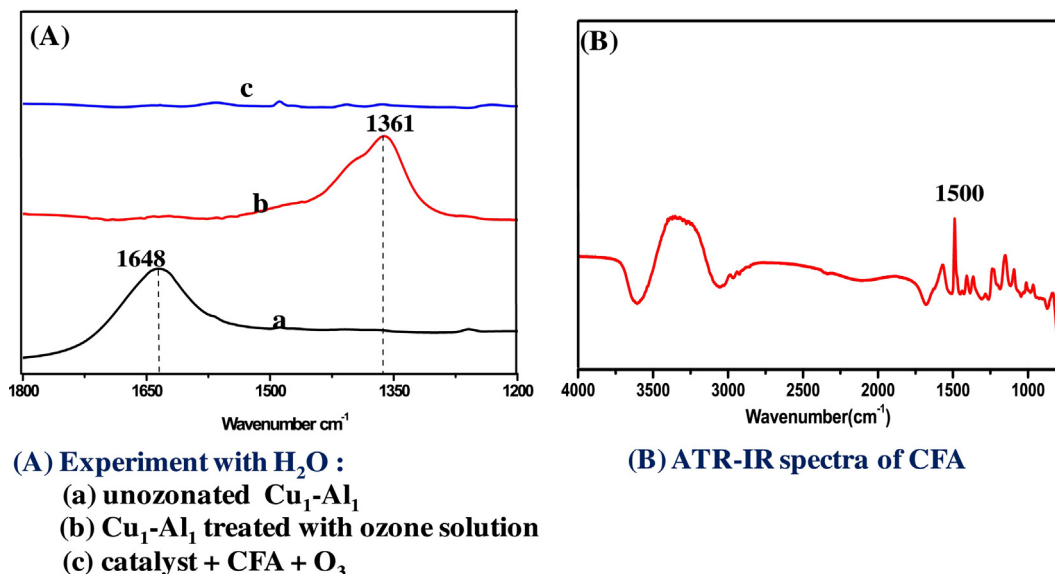


**Fig. 2.** (A) ATR-IR spectra of  $\text{Cu}_1\text{-Al}_1$  (ca.50 mg) with and without ozone in presence of  $\text{H}_2\text{O}$  and (B) ATR-IR spectra of CFA.

TOC removal at pH 7 and 10, respectively, in 2 h ozonation when compared to the reaction at free pH (see Table 1 and Fig. 1). Consequently, the mineralization efficiency was enhanced for initial pH values between 7 and 10.

### 3.6. The investigation of active sites by *in situ* ATR-IR

The  $\text{Cu}_1\text{-Al}_1$  catalyst showed very good performance in the degradation and mineralization of CFA in catalytic ozonation without detectable leaching of copper. In order to identify surface active species formed during the reaction on this  $\text{Cu}_1\text{-Al}_1$  catalyst and the interaction with ozone, *in situ* ATR-IR spectroscopy was used to study the surface changes occurring on the catalyst. For that purpose several experiments were carried out by subsequent passing water solutions of ozone and phosphate over the catalyst.

According to the literature [67,68], it is assumed that there is an interaction between ozone and the surface species generated from dissociative adsorption of water molecule on Lewis acid sites. Then, the generation of reactive oxygen species is initiated, which help for the degradation of organic pollutants. According to ozone decomposition mechanism studies in gas phase, both Bronsted and Lewis acid sites are considered to be catalytic centres on the catalyst surface [63]. Lewis bases like water and ozone can adsorb on the catalyst surface because of the presence of strong Lewis acid sites on e.g. alumina [69,70].

Resulting spectra of *in situ* ATR-IR measurements of  $\text{H}_2\text{O}$ ,  $\text{Cu}_1\text{-Al}_1$  with  $\text{H}_2\text{O}$  and  $\text{Cu}_1\text{-Al}_1$  treated with ozone solution are shown in Fig. 9S. Spectrum of  $\text{H}_2\text{O}$  has characteristic stretching vibration mode at frequency around  $3390 \text{ cm}^{-1}$  and a bending vibration mode at  $1648 \text{ cm}^{-1}$ , as shown in Fig. 9S(a). However, after the addition of aqueous ozone on the layer of catalyst, a new peak appeared at  $1361 \text{ cm}^{-1}$  [see Fig. 9S(c)]. Roscoe and Abbott also observed this type of peak on the surface of alumina treated with aqueous solution of ozone [71] and they confirmed that this peak belonged to new oxide species formed by interaction of ozone and Lewis acid sites on the surface of the catalyst. Similar surface species were also found on the ozonated  $\text{MnO}_x/\text{Al}_2\text{O}_3$  [72,73]. This suggests that it likely belongs to surface oxide species formed on the catalyst with aqueous ozone.

The reference spectrum of CFA was measured by passing CFA aqueous solution over the catalyst surface, and an intense peak of CFA around  $1500 \text{ cm}^{-1}$  was observed (see Fig. 2B). When CFA solu-

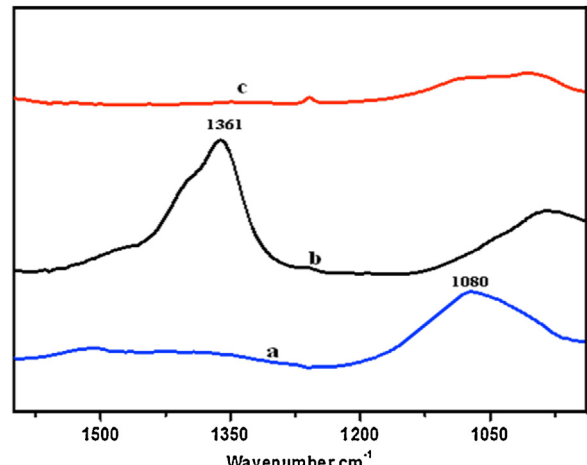


**Fig. 3.** *In situ* ATR-IR spectra of (a) phosphate (30 mM), (b)  $\text{Cu}_1\text{-Al}_1$  treated with  $\text{O}_3$  and (c)  $\text{Cu}_1\text{-Al}_1$  (ca.50 mg) treated with ozone and phosphate (30 mM) solution.

tion was passed on the catalyst surface after having passed aqueous ozone, the spectral feature band at  $1361 \text{ cm}^{-1}$  disappeared, as can be seen in Fig. 2A(c). Moreover, all peak intensities of CFA and particularly peak at  $1500 \text{ cm}^{-1}$  from the acidic groups decreased when compared to reference spectra of CFA. These results indicate that active species on catalyst surface play an important role in the degradation of clofibric acid in ozonation process. *In situ* ATR-IR experiments indicated a strong interaction between ozone and the surface of the catalyst in presence of water, subsequently surface active species is generated, which would enhance ozone decomposition and thus promoting hydroxyl radical generation.

Phosphate can be strongly bonded with the surface Lewis acid sites of the catalyst, as it is a stronger base than water [36,67]. In presence of phosphate, the adsorption of ozone on catalyst surface would be then prevented. For this reason, the effect of phosphate was investigated in the interaction of  $\text{Cu}_1\text{-Al}_1$  with ozone. Fig. 3a shows the spectra of phosphate on the catalyst surface and a spectral band appeared at  $1080 \text{ cm}^{-1}$ , belonging to phosphate vibration. Fig. 3b shows the spectra of ozone on the catalyst surface, presenting absorption peak of active species (at  $1361 \text{ cm}^{-1}$ ), as commented before. When phosphate solution was passed over the ozonated

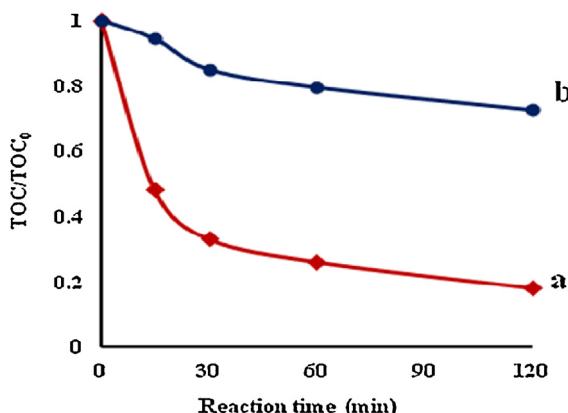


**Fig. 4.** Effect of phosphate on the activity of Cu<sub>1</sub>-Al<sub>1</sub> (a) without phosphate and (b) with 5 mM phosphate (reaction conditions: 500 mL, [CFA]<sub>0</sub> = 100 mg/L, O<sub>3</sub> production = 1.2 g/h, O<sub>2</sub> flow rate = 40 L/h, catalyst concentration = 0.5 g/L, Temp. = R.T., pH = free).

surface, the peak at 1361 cm<sup>-1</sup> disappeared (Fig. 3c). The presence of phosphate in the solution seems to inhibit the interaction of ozone with catalyst surface. This observation demonstrates that Lewis acidic sites of catalysts are responsible for the formation of surface active species.

To check the effect of phosphate on the catalytic activity, tests in presence and absence of phosphate were performed. TOC removal was greatly suppressed when catalytic ozonation experiment was performed in the presence of 5 mM phosphate (see Fig. 4b), achieving yields similar to those obtained by single ozonation. The results indicate therefore that in presence of phosphate, catalytic role of Cu<sub>1</sub>-Al<sub>1</sub> was almost completely suppressed.

The highest activity and stability of calcined Cu<sub>1</sub>-Al<sub>1</sub> for CFA degradation and mineralization could be then related to the presence of stronger Lewis acidic sites than the other Cu-catalysts, as shown by ammonia TPD results (see Fig. 6S). Also higher copper loading in Cu<sub>1</sub>-Al<sub>1</sub> and high dispersion of Cu species on the surface of this catalyst can play a role on this higher activity. Ozone has nucleophilic and electrophilic sites as it is a dipole molecule [74]. During the interaction, ozone may combine with the H (electrophilic) and O (nucleophilic) atoms of surface hydroxyl group of the catalyst. This can result in faster radical generation because of enhancement of ozone decomposition. These results suggest that in the catalytic ozonation process in presence of water, the reaction of ozone with the adsorbed water layer that interact with the surface of the catalyst, generates activated species that plays an important role in the catalytic behaviour.

#### 4. Conclusions

Clofibric acid can be effectively degraded by catalytic ozonation using different Cu-based catalysts with improved stability and activity. The results of this study indicate that copper hydrotalcite, Cu-spinel, copper dawsonite and Cu<sub>1</sub>-Al<sub>1</sub> oxide catalysts are suitable and highly active catalysts in the ozonation of clofibric acid solutions.

Among all tested Cu-based catalysts for CFA degradation, Cu<sub>1</sub>-Al<sub>1</sub> exhibited excellent activity, in which even at low calcination temperature (400 °C) distinct spinel CuAl<sub>2</sub>O<sub>4</sub> phase was formed. In the presence of Cu<sub>1</sub>-Al<sub>1</sub> oxide catalyst, 82% and 96% mineralization was observed after 2 and 6 h of ozonation of CFA, without any leaching of copper. Moreover, after being reused three times, Cu<sub>1</sub>-Al<sub>1</sub> still showed excellent activity, maintaining 76% mineralization after 2 h of ozonation. These results suggested that Cu<sub>1</sub>-Al<sub>1</sub> catalyst possess a high activity and stability in ozonation.

By means of the experiments performed with *in situ* ATR-IR technique, it can be concluded that there is a strong interaction between ozone and the surface of catalyst Cu<sub>1</sub>-Al<sub>1</sub> in presence of water. Due to this, surface-active species are generated, which would enhance ozone decomposition and thus promoting hydroxyl radical generation. Phosphate, a stronger base than water, was used to prevent the adsorption of ozone on the surface of the catalyst demonstrating the necessity of the ozone adsorption on the catalytic surface. This is also demonstrated by the results of TOC removal, which is very much suppressed in presence of phosphate.

#### Acknowledgments

This work was funded by the Spanish Ministry of Science and Innovation (MICINN), project CTQ2012-35789-C02-02. S.S. acknowledges Universitat Rovira i Virgili for the PhD grant. Authors gratefully acknowledge Dr. A. Urakawa, Institute of Chemical Research of Catalonia (ICIQ), Tarragona, for the use of equipment for *in situ* ATR-IR characterization of catalyst and the related scientific discussions. F. M. would like to thank ICREA Academia for funding support.

#### Appendix A. Supplementary data

Supplementary data associated with this article can be found, in the online version, at <http://dx.doi.org/10.1016/j.apcatb.2017.02.071>.

#### References

- [1] C.C.A. Loures, M.A.K. Alcântara, H.J.I. Filho, A.C.S.C. Teixeira, F.T. Silva, T.C.B. Paiva, G.R.L. Samanamud, *Int. Rev. Chem. Eng.* 5 (2) (2013) 102–120.
- [2] P.M. Álvarez, J. Jaramillo, F. López-Pinero, P.K. Plucinski, *Appl. Catal. B: Environ.* 100 (2010) 328–345.
- [3] S.K. Khetan, T.J. Collins, *Chem. Rev.* 107 (2007) 2319–2364.
- [4] S. Zuehlke, U. Duennbier, T. Heberer, *Anal. Chem.* 76 (2004) 6548–6554.
- [5] D.W. Kolpin, E.T. Furlong, M.T. Meyer, E.M. Thurman, S.D. Zaugg, *Environ. Sci. Technol.* 36 (1999–2000) 1202–1211.
- [6] S.K. Behera, H.W. Kim, J.E. Oh, H.S. Park, *Sci. Total Environ.* 40 (2011) 4351–4360.
- [7] H.-C. Chen, P.-L. Wang, W.-H. Ding, *Chemosphere* 72 (2008) 863–869.
- [8] Q. Sui, J. Huang, S. Deng, G. Yu, Q. Fan, *Water Res.* 44 (2010) 417–426.
- [9] D. Camacho-Muñoz, J. Martín, J.L. Santos, I. Aparicio, E. Alonso, *J. Hazard. Mater.* 183 (2010) 602–608.
- [10] A. Tauxe-Wuersch, L.F. DeAlencastro, D. Grandjean, J. Tarradellas, *Water Res.* 39 (2005) 1761–1772.
- [11] P.H. Roberts, K.V. Thomas, *Sci. Total Environ.* 356 (2006) 143–153.
- [12] S. Weigel, J. Kuhlmann, H. Hühnerfuss, *Sci. Total Environ.* 295 (2002) 131–141.
- [13] B. Ferrari, N. Paxéus, R. LoGiudice, A. Pollio, J. Garric, *Ecotoxicol. Environ. Saf.* 55 (2003) 359–370.
- [14] M.D. Hernando, A. Agüera, A.R. Fernández-Alba, *Anal. Bioanal. Chem.* 387 (2007) 1269–1285.
- [15] P. Verlicchi, M. AlAuikidý, E. Zambello, *Sci. Total Environ.* 429 (2012) 123–155.
- [16] R. Salgado, A. Oehmen, J.P. Noronha, M.A.M. Reis, *J. Hazard Mater.* 241–242 (2012) 182–189.
- [17] M. Winkler, J.R. Lawrence, T.R. Neu, *Water Res.* 35 (2001) 3197–3205.
- [18] V. Matamoros, J. García, J.M. Bayona, *Water Res.* 42 (2008) 653–660.
- [19] A. Dordio, A.J. palace Carvalho, D.M. Teixeira, C.B. Dias, A.P. Pinto, *Bioresour. Technol.* 101 (2010) 886–892.
- [20] T.A. Ternes, Occurrence of drugs in German sewage treatment plants and rivers, *Water Res.* 32 (1998) 3245–3260.
- [21] A. Joss, S. Zabczyński, A. Göbel, B. Hoffmann, D. Löffler, C.S. Mc Ardell, T.A. Ternes, A. Thomsen, H. Siegrist, *Water Res.* 40 (2006) 1686–1696.
- [22] F. Gagne, C. Blaise, C. Andre, *Ecotoxicol. Environ. Saf.* 64 (2006) 329–336.
- [23] B. Halling-Sørgaen, S.N. Lanzky, F. Ingerslev, H.C. Holten, S.E. Jørgensen, *Chemosphere* 36 (1998) 357–394.
- [24] C. Tixier, P. Heinz, S.S. Oellers, S.R. Muller, *Environ. Sci. Technol.* 37 (2003) 1061–1068.
- [25] H.-R. Buser, M.D. Müller, N. Theobald, *Environ. Sci. Technol.* 32 (1998) 188–192.
- [26] J.P. Embilidge, M.E. DeLorenzo, *Environ. Res.* 100 (2006) 216–226.
- [27] T. Heberer, H.J. Stan, *Int. J. Environ. Anal. Chem.* 67 (1997) 113–124.
- [28] C. Tixier, H.P. Singer, S. Oellers, S.R. Muller, *Environ. Sci. Technol.* 37 (2003) 1061–1068.

[29] J.H. Ramirez, C.A. Costa, L.M. Maderia, G. Mata, M.A. Vicente, M.L. Rojas-Cervantes, A.J. Lopez-Peinado, R.M. Martin-Aranda, *Appl. Catal. B: Environ.* 71 (2007) 44–56.

[30] S. Contreras, M. Rodriguez, F. Al Momani, C. Sans, S. Esplugas, *Water Res.* 37 (2003) 3164–3171.

[31] T.A. Terens, M. Meisenheimer, D. McDowell, F. Sacher, H.J. Brauch, *Environ. Sci. Technol.* 36 (2002) 3855–3863.

[32] C. Zwiener, F.H. Frimmel, *Water Res.* 34 (2000) 1881–1885.

[33] W. Hua, E.R. Bennett, R.J. Letcher, *Water Res.* 40 (2006) 2259–2266.

[34] C. Canton, S. Esplugas, J. Casado, *Appl. Catal. B: Environ.* 43 (2003) 139–149.

[35] D. Hofbauer, S.A. Andrews, *Water Sci. Technol.: Water Supply* 4 (2004) 41–46.

[36] L. Yang, C. Hu, Y. Nie, J. Qu, *Environ. Sci. Technol.* 43 (2009) 2525–2529.

[37] R. Rosal, M.S. Gonzalo, A. Rodriguez, E. Garcia-Calvo, J. Hazard. Mater. 183 (2010) 271–278.

[38] E.C. Chetty, S. Maddila, C. Southway, S.B. Jonnalagadda, *Ind. Eng. Chem. Res.* 51 (2012) 2864–2873.

[39] M. Sui, S. Xing, L. Sheng, S. Huang, H. Guo, *J. Hazard. Mater.* 227–228 (2012) 227–236.

[40] Y. Guo, Li Yang, X. Cheng, X. Wang, *Environ. Anal. Toxicol.* 2 (2012) 7.

[41] L. Yang, C. Hu, Y. Nie, J. Qu, *Appl. Catal. B: Environ.* 97 (2010) 340–346.

[42] C. Cooper, R. Burch, *Water Res.* 33 (1999) 3695–3700.

[43] Q. Jiuhui, L. Haiyan, L. Huijuan, H. Hong, *Catal. Today* 90 (2004) 291–296.

[44] R. Allmann, H.H. Lohse, N. Jb. Min. 11 (1966) 161–180.

[45] P. Konova, M. Stoyanova, A. Naydenov, S. Christoskova, D. Mehandjiev, *Appl. Catal. A* 298 (2006) 109–114.

[46] H. Einaga, A. Ogata, *J. Hazard. Mater.* 164 (2009) 1236–1241.

[47] H. Einaga, S. Futamura, *React. Kinet. Catal. Lett.* 81 (2004) 121–128.

[48] A. Mashayekh-Salehi, G. Moussavi, K. Yaghmaeian, *Chem. Eng. J.* 310 (2017) 157–169.

[49] R. Yin, W. Guo, X. Zhou, H. Zheng, J. Du, Q. Wu, J. Chang, N. Ren, *RSC Adv.* 6 (2016) 19265–19270.

[50] G. Gao, J. Shen, W. Chu, Z. Chen, L. Yuan, *Sep. Purif. Technol.* 173 (2017) 55–62.

[51] M.S. Yalfani, S. Contreras, J. Llorca, F. Medina, *Appl. Catal. B: Environ.* 107 (2011) 9–17.

[52] S.S. Sable, S. Contreras, F. Medina, *Appl. Catal. B: Environ.* 150–151 (2014) 30–36.

[53] W. Li, G. Gibbs, S. Oyama, *J. Am. Chem. Soc.* 120 (1998) 9041–9046.

[54] R. Radhakrishnan, S.T. Oyama, Y. Ohminami, K. Asakura, *J. Phys. Chem. B* 105 (38) (2001) 9067–9070.

[55] K.M. Bulanin, J.C. Lavalle, A.A. Tsyanenko, *Colloids Surf. A* 101 (2–3) (1995) 153–158.

[56] J. Ma, N.J.D. Graham, *Water Res.* 33 (3) (1999) 785–793.

[57] T. Zhang, C. Li, J. Ma, H. Tian, Z. Qiang, *Appl. Catal. B* 82 (1–2) (2008) 131–137.

[58] Y. Joseph, W. Ranke, W. Weiss, *J. Phys. Chem. B* 104 (14) (2000) 3224–3236.

[59] M. Ernst, F. Lurot, J.C. Schrotter, *Appl. Catal. B: Environ.* 47 (2004) 15–25.

[60] J.S. Park, H. Choi, J. Cho, *Water Res.* 38 (2004) 2285–2292.

[61] R. Andreozzi, A. Insola, V. Caprio, R. Marotta, V. Tufano, *Appl. Catal. A: Gen.* 138 (1996) 75–81.

[62] F.J. Beltran, F.J. Rivas, R. Montero-de-Espinosa, *Ind. Eng. Chem. Res.* 42 (2003) 3218–3224.

[63] B. Kasprzyk-Hordern, M. Zioek, J. Nawrocki, *Appl. Catal. B* 46 (4) (2003) 639–669.

[64] J. Lin, A. Kawai, T. Nakajima, *Appl. Catal. B: Environ.* 39 (2002) 157–165.

[65] R.B. Mane, A.M. Hengane, A.A. Ghalwadkar, V. Subramanian, P.H. Mohite, H.S. Potdar, C.V. Rode, *Catal. Lett.* 135 (2010) 141–147.

[66] T.R. Hughes, H.M. White, *J. Phys. Chem.* 71 (1967) 2192–2201.

[67] A.H. Lv, C. Hu, Y.L. Nie, J.H. Qu, *Appl. Catal. B* 100 (2010) 62–67.

[68] W.W. Li, Z.M. Qiang, T. Zhang, F.L. Cao, *Appl. Catal. B* 113–114 (2012) 290–295.

[69] K.M. Bulanin, J.C. Lavalle, A.A. Tsyanenko, *Colloids Surf. A* 101 (2–3) (1995) 153–158.

[70] H.A. Al-Abadleh, V.H. Grassian, *Langmuir* 19 (2) (2003) 341–347.

[71] J.M. Roscoe, J.P.D. Abbott, *J. Phys. Chem. A* 109 (2005) 9028–9034.

[72] F.J. Beltran, J. Rivas, P. Alvarez, R. Montero-de-Espinosa, *Ozone Sci. Eng.* 24 (2002) 227–237.

[73] T.X. Sheng, H. Chun, H.Q. Jiu, H. Hong, Y. Min, *Environ. Sci. Technol.* 42 (2008) 3363–3368.

[74] F.J. Beltran, *Ozone Reaction Kinetics for Water and Wastewater Systems*, Lewis Publisher, Boca Raton, 2017, pp. 3–4 (published December 29, 2003).